

Supplemental Material

Extensive evidence for the Last Interglacial analog of the glacial outburst event 8,200 years ago

Yuxin Zhou^{1,2}, Jerry McManus^{1,2}

¹Lamont-Doherty Earth Observatory of Columbia University, Palisades, NY 10964, USA

²Dept. of Earth and Environmental Sciences, Columbia University, New York, NY 10027, USA

Text S1 - Identification of the red layer

Sediment color has aided in the study of the chemical composition and provenance of deep-sea sediments (Barranco et al., 1989; Balsam, 1991; Bond et al., 1992; Adkins et al., 1997; Boyle, 2000; Giosan et al., 2001, 2002a, 2002b; Keigwin, 2001; Balsam et al., 2007; Leng et al., 2018). The lighting condition and the camera used may bias the core photos, so visually identifying the red layer is inevitably subjective. We therefore use a^* , a measure of the green to red color spectrum, to aid the identification (Blum, 1997). Additionally, during core photo examinations, we found red-colored sediments to be rare and easily distinguished from the background sediments. Even rarer are red sediment layers with a sharp basal contact with underlying sediments, which implies rapid deposition. Identification of any potential red layer in the study interval is aided by the fact that interglacial sediments are typically lighter in color, reflecting the higher CaCO_3 content and making the red sediments further stand out.

Text S2 – Chronology of EW37JPC

Core EW37JPC was subsampled at 2 cm intervals over the interval 777-1330 cm. The samples were freeze-dried, weighed, placed in deionized water, and spun for an hour. The wet samples were washed through 63 μm sieves, and the coarse fraction retained in the sieves was dried, weighed, and transferred to glass vials. The coarse fraction was dry sieved at $>150 \mu\text{m}$, from which the *Cibicidoides wuellerstorfi* tests were picked. The $\delta^{18}\text{O}$ measurements on *Cibicidoides wuellerstorfi* tests were conducted with a Thermo Delta V Plus gas-source isotope-ratio mass spectrometer equipped with a Kiel IV individual acid-bath sample preparation device at the Lamont-Doherty Earth Observatory of Columbia University stable isotope laboratory. The long-term standard deviation of measurements made on standard carbonate NBS19 was 0.06 ‰. One

to three separate stable isotope analyses were at each depth except when the abundance of *Cibicidoides wuellerstorfi* was low. When duplicates were available, the average was presented for each sample.

The chronostratigraphy of EW37JPC was established by aligning our benthic $\delta^{18}\text{O}$ record to the Prob-stack using the open-source HMM-Stack software (<https://github.com/seonminahn/HMM-Stack>) (Ahn et al., 2017). The Prob-stack compiles 123 additional published benthic records to those included in the LR04 stack (Lisiecki and Raymo, 2005). It uses a profile hidden Markov Model (HMM) to build a probabilistic stack with age uncertainty estimates. Compared to the conventional graphical correlation method (Paillard et al., 1996), this probabilistic approach allows for a better assessment of the uncertainty of our age model (Fig. S1).

Text S3 - NAMOC tracing

We considered the potential role of the regional bathymetrical setting in propagating the red layer. A prominent geological feature in the northwest Atlantic is the Northwest Atlantic Mid-Ocean Channel (NAMOC). First discovered in the 1950s (Ewing et al., 1953), the NAMOC has been studied in much detail (Chough and Hesse, 1976; Hesse and Rakofsky, 1992; Hesse et al., 1997; Klaucke et al., 1998; Skene et al., 2002). A recent mapping campaign promises to map even more morphologic details of the NAMOC with modern technologies (Krastel and Mosher, 2022). However, as far as we know, only one digitalized version of the geological feature is publicly available. It is a version that ignores the feature's southern half (GEBCO Subcommittee on Undersea Feature Names, 2015). We digitalized the feature using a combination of the GEBCO bathymetry dataset (GEBCO Bathymetric Compilation Group, 2019) and the published maps depicting the feature (Ewing et al., 1953; Chough and Hesse, 1976; Stoner et al., 1996; Klaucke et al., 1998; Rashid et al., 2003b, 2003a). However, the bathymetry dataset's resolution did not allow us to trace the complex tributaries of the NAMOC. An Esri™ shapefile is made available for download.

Text S4 – Red layer alignment in cores

In IODP U1302 and U1305, the red layer can be dated to about 126 ka (Nicholl et al., 2012). Although this age is based on planktic $\delta^{18}\text{O}$, which can be influenced by the surface water density, this age is supported by paleointensity measurements at U1302 (Channell et al., 2012).

A recent study dated the red layer in U1302 and U1305 based on the alignments of % *Neogloboquadrina pachyderma*, Modern Analog Technique (MAT) sea surface temperatures, ice-rafted debris (percentage and concentration), and planktic $\delta^{18}\text{O}$, and arrived at an age of 126.5 ka for the red layer (Hume, 2018).

In ODP 646, where the age model is also based on planktic $\delta^{18}\text{O}$, the red layer's age is given as about 130.5 ka (Aksu and Hillaire-Marcel, 1989; Hillaire-Marcel et al., 1990).

In ODP 1063, the age model is based on the alignment of Ti/Ca to a Greenland ice core record (Böhm et al., 2015), which puts the red layer at 120.5 ka. The ODP 1063 age model was hampered by fewer variations of Ti/Ca around the red layer, which may add uncertainty to the alignment points.

We do not include MD03-2664 (57°26.34'N, 48°36.35'W; 3440 m water depth) in our discussion because it is not a drill core, and its core images are not publicly available. Additionally, MD03-2664 is only a short distance away from U1305 (both are located on the Eirik Drift). Nevertheless, for the sake of completeness, we briefly review the red sediment layer that has been discovered in this core. The red layer was found in the core and dated to be 124.2-124.7 kyrs old based on benthic $\delta^{18}\text{O}$ (Galaasen et al., 2014). The red layer in the core was found to be deposited during a surface cooling event during 124-126 ka identified earlier (Irvali et al., 2012). In MD03-2664, the red layer was also correlated with Cooling Event 27 (C27) and was dated to be 125.7-126.2 kyrs old based on its alignment to ODP984, whose age model was created by alignment to MD01-2444. The age model of MD01-2444 was in turn based on alignment with a Corchia Cave speleothem $\delta^{18}\text{O}$ record (Tzedakis et al., 2018).

Text S5 – LILO event duration estimate

The duration of time represented by the deposition of the red layer in EW37JPC can be estimated by $^{230}\text{Th}_{\text{xs}}$ profiling, a technique previously employed to estimate the durations of Heinrich events (Francois and Bacon, 1994; McManus et al., 1998). The assumption of $^{230}\text{Th}_{\text{xs}}$ profiling is that the accumulated inventory of $^{230}\text{Th}_{\text{xs}}$ is proportional to the time passed between sediment horizons. This is because $^{230}\text{Th}_{\text{xs}}$ is inversely related to mass flux and mass flux is inversely

related to the time pass between sediment horizons. The major source of uncertainty is how we define the red layer (Fig. S2). First, we can define the red layer by the midpoints between the high Fe flux data point and the surrounding low mass flux data points (1217.5 – 1222.5 cm). The estimated duration of the deposition of the red layer based on $^{230}\text{Th}_{\text{xs}}$ profiling is 126 years. The estimate based on the benthic $\delta^{18}\text{O}$ age model is 400 years. Second, we can define the red layer by the peak of the Ca/Sr data (1196 – 1233 cm). By this definition, the duration of the red layer is 4043 years based on $^{230}\text{Th}_{\text{xs}}$ profiling and 3800 years based on the age model. We consider both methods of estimation to be the upper limits of the duration of the respective definition of the red layer. For $^{230}\text{Th}_{\text{xs}}$ profiling, potential sediment mixing by bioturbation means the true $^{230}\text{Th}_{\text{xs}}$ of the red layer is likely even lower than we measured. For the duration estimate based on the age model, the relatively invariant benthic $\delta^{18}\text{O}$ during MIS 5e means that the age model may not fully capture rapid deposition events. Because our duration estimates are upper limits, they are in line with the 8.2-ka event duration estimate of 160.5 years based on ice core data (Thomas et al., 2007).

Text S6 – Implication for the LIS extent during the LIG

Does the higher-than-today sea level during the LIG allow a substantial LIS presence?

Unfortunately, this is not a question easily resolvable by looking at global mean sea level (GMSL). While GMSL can be used to assess the global ice volume changes (provided that other parameters are controlled), it cannot clarify how the ice volume changes were distributed among ice sheets. Case in point, GMSL was established to be 2-4.5 m during 125 ka (Kopp et al., 2009; Dyer et al., 2021) and -14 m during 8.2 ka (Lambeck et al., 2014). Nominally, up to 18.5 m sea level equivalent less ice volume existed during 125 ka compared to 8.2 ka. However, it is unclear how the sea level equivalent ice volume was distributed among the various ice sheets at 125 ka.

Ice modeling specific to the Laurentide and constrained by observation, such as Tarasov et al. (2012), can elucidate the LIS ice volume changes. However, such an exercise has not been done for the LIG, as far as we are aware. This is likely due to a lack of knowledge of the LIS extent during MIS 5e, as past interglacial ice extents are generally difficult to reconstruct due to erosion by subsequent glacial advances (Dalton et al., 2020).

We note that in Kopp et al. (2009)'s GMSL reconstruction, the event occurred during the upward sea level trend toward its peak, and not after that was achieved. This estimated upward GMSL trend allows the possibility that the LIS persisted and was in an ongoing melting stage. The uncertainty associated with event's age furthers the potential consistency of that scenario. However, as we have discussed, at this point we simply do not know which ice sheet(s) was responsible for the GMSL rise at 125 ka.

Core	Longitude (°)	Latitude (°)	Depth (m)	Age model	Core photo link	Red layer
IODP U1305	-48.5203	57.4672	3463	(Nicholl et al., 2012)	http://publications.iodp.org/proceedings/303_306/EXP_REPT/CORES/IMAGES/1305C4H.PDF	C4H2 30 cm (22.20 mcd)
IODP U1302	-45.6463	50.1547	3569	(Channell et al., 2012)	http://publications.iodp.org/proceedings/303_306/EXP_REPT/CORES/IMAGES/1302C2H.PDF http://publications.iodp.org/proceedings/303_306/EXP_REPT/CORES/IMAGES/1302A2H.PDF http://publications.iodp.org/proceedings/303_306/EXP_REPT/CORES/IMAGES/1302B2H.PDF	C2H6 100 cm (22.05 mcd); A2H6 5 cm; B2H2 142.5 cm
EW37JPC	-46.28	43.68	3981	(Zhou et al., in review)	This study	1220 cm
ODP 980	-14.7022	55.4848	2172	(Oppo et al., 2006)	http://www-odp.tamu.edu/publications/162_IR/VOLUME/CORES/IMAGES/980A2H.PDF	N/A
ODP 646	-48.3691	58.2093	3440	(Aksu and Hillaire-Marcel, 1989; Hillaire-Marcel et al., 1990)	http://www-odp.tamu.edu/publications/105_IR/VOLUME/CORES/IMAGES/646B2H.PDF	B2H5 24 cm
ODP 647	-45.262	53.3313	3869	(Aksu et al., 1989)	http://www-odp.tamu.edu/publicati	N/A

					ons/105_IR/VOLUME/CORES/IMAGES/647B1H.PDF	
ODP 1063	-57.615	33.6867	4584	(Böhm et al., 2015)	http://www-odp.tamu.edu/publications/172_IR/CORES/IMAGES/1063D5H.PDF http://www-odp.tamu.edu/publications/172_IR/CORES/IMAGES/1063A4H.PDF http://www-odp.tamu.edu/publications/172_IR/CORES/IMAGES/1063B4H.PDF http://www-odp.tamu.edu/publications/172_IR/CORES/IMAGES/1063C5H.PDF	D5H2 100 cm (35.84 mcd); A4H5 65 cm (32.71 mcd); B4H5 25 cm (35.93 mcd) C5H1 75 cm (35.70 mcd)
IODP U1313	-32.9532	41.002	3412	(Smith et al., 2013)	http://publications.iodp.org/proceedings/303_306/EXP_REPT/CORES/IMAGES/1313A2H.PDF	N/A
IODP U1314	-27.8865	56.352	2799	(Alvarez Zarikian et al., 2009)	http://publications.iodp.org/proceedings/303_306/EXP_REPT/CORES/IMAGES/1314A3H.PDF	N/A
ODP 1059	-75.4188	31.6744	2985	(Oppo et al., 2001)	http://www-odp.tamu.edu/publications/172_IR/CORES/IMAGES/1059A5H.PDF	N/A
ODP 1060	-74.4665	30.76	3481	(Grützner et al., 2002)	http://www-odp.tamu.edu/publications/172_IR/CORES/IMAGES/1060A4H.PDF	N/A
ODP 1061	-73.5999	29.975	4047	(Grützner et al., 2002)	http://www-odp.tamu.edu/publications/172_IR/CORES/IMAGES/1061D4H.PDF http://www-odp.tamu.edu/publications/172_IR/CORES/IMAGES/1061C4H.PDF	D4H7 45 cm (34.22 mcd); C4H5 110 cm (34.39 mcd)
ODP 1062	-74.407	28.2464	4763	(Bourne et al., 2012)	http://www-odp.tamu.edu/publications/172_IR/CORES/IMAGES/1062A4H.PDF	N/A

					ons/172_IR/CORES/IMAGES/1062E3H.PDF	
IODP U1304	-33.5203	53.0505	3069	(Hodell et al., 2009)	http://publications.iodp.org/proceedings/303_306/EXP_REPT/CORES/IMAGES/1304A2H.PDF	N/A
ODP 983	-23.6406	60.4033	1983	(Hodell et al., 2009)	http://www-odp.tamu.edu/publications/162_IR/VOLUME/CORES/IMAGES/983A2H.PDF	N/A
ODP 919	-37.4602	62.67	2088	(Flower, 1998)	http://www-odp.tamu.edu/publications/152_IR/VOLUME/CORES/IMAGES/919A3H.PDF	N/A

Table S1. Cores examined for the presence of a red layer during the LIG.

Core	Longitude (°)	Latitude (°)	Reference
HU90023-085	-76.38	62.62	(Barber et al., 1999)
HU90023-101	-74.3	63.05	(Kerwin, 1996; Barber et al., 1999)
HU90023-099	-74.57	63.07	(Barber et al., 1999)
HU85027-068	-74.31	63.08	(Barber et al., 1999)
HU93034-004	-66.43	61.22	(Barber et al., 1999)
HU90023-045	-66.14	60.95	(Kerwin, 1996; Barber et al., 1999)
HU90023-064	-70.58	61.13	(Barber et al., 1999)
HU85027-057	-66.43	61.07	(Barber et al., 1999)
HU93034-004	-66.43	61.22	(Barber et al., 1999)
HU90023-045	-66.14	60.95	(Barber et al., 1999)
HU92023-157	-66.13	60.95	(Andrews et

			al., 1995)
HU93034-002	-65.70	60.95	(Jennings et al., 1998)
HU93034-004	-66.43	61.22	(Jennings et al., 1998)
MD99-2236	-56.18	54.62	(Jennings et al., 2015)
AMD0509-28PC	-74.30	63.05	(St-Onge and Lajeunesse, 2007)
AMD0509-27bLEH	-86.21	61.05	(St-Onge and Lajeunesse, 2007)
MSM45-19-2	-61.94	58.76	(Lochte et al., 2019)

Table S2. Cores documented with the occurrence of a red layer during the 8.2-ka event.

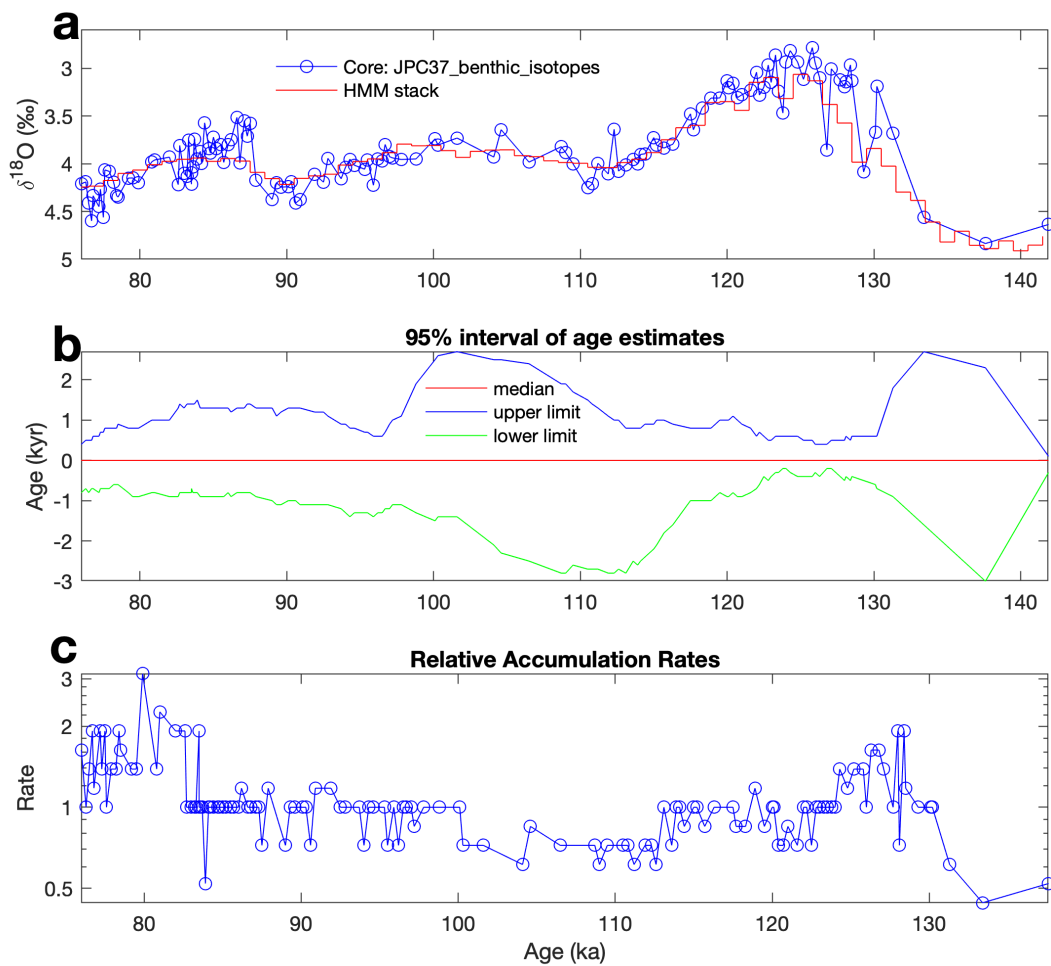


Figure S1. The chronology of EW37JPC as established by fitting our benthic $\delta^{18}\text{O}$ record to the Prob-stack. (a) The benthic $\delta^{18}\text{O}$ of EW37JPC (blue) and Prob-stack (red). (b) Confidence intervals of the chronology. (c) Relative accumulation rates based on the chronology (accumulation rate of 1 means the accumulation rate at a certain depth is equal to the average accumulation rate of the whole segment of the core).

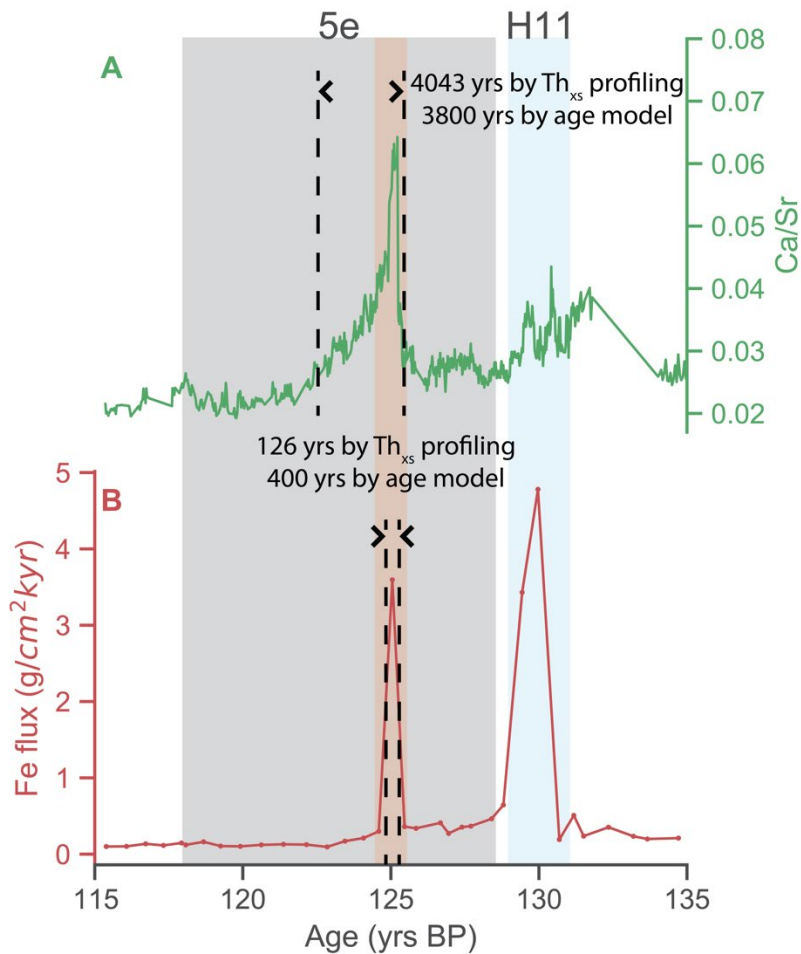


Figure S2. Estimates of the duration of the LIL0 event. (A) Two methods of duration estimates if the red layer is defined by the Ca/Sr peak. (B) Two methods of duration estimates if the red layer is defined by the Fe flux peak.

References

- Adkins, J.F., Boyle, E.A., Keigwin, L., and Cortijo, E., 1997, Variability of the North Atlantic thermohaline circulation during the last interglacial period: *Nature*, v. 390, p. 154–156, doi:10.1038/36540.
- Ahn, S., Khider, D., Lisiecki, L.E., and Lawrence, C.E., 2017, A probabilistic Pliocene–Pleistocene stack of benthic $\delta^{18}\text{O}$ using a profile hidden Markov model: *Dynamics and Statistics of the Climate System*, v. 2, doi:10.1093/climsys/dzx002.
- Aksu, A.E., and Hillaire-Marcel, C., 1989, (Appendix B) Oxygen and carbon isotope ratios of planktonic foraminifera of ODP Site 105-646: , p. 1263 data points, doi:10.1594/PANGAEA.744961.
- Aksu, A.E., de Vernal, A., and Mudie, P.J., 1989, High-resolution foraminifer, palynologic, and stable isotopic records of upper pleistocene sediments from the Labrador Sea: paleoclimatic and paleoceanographic trends: v. 105, doi:10.2973/odp.proc.sr.105.1989.
- Alvarez Zarikian, C.A., Stepanova, A.Yu., and Grützner, J., 2009, Glacial–interglacial variability in deep sea ostracod assemblage composition at IODP Site U1314 in the subpolar North Atlantic: *Marine Geology*, v. 258, p. 69–87, doi:10.1016/j.margeo.2008.11.009.
- Andrews, J.T., Maclean, B., Kerwin, M., Manley, W., Jennings, A.E., and Hall, F., 1995, Final stages in the collapse of the laurentide ice sheet, Hudson Strait, Canada, NWT: 14C AMS dates, seismics stratigraphy, and magnetic susceptibility logs: *Quaternary Science Reviews*, v. 14, p. 983–1004, doi:10.1016/0277-3791(95)00059-3.
- Balsam, W., 1991, Sediment dispersal in the Atlantic Ocean: evaluation by visible light spectra: *Reviews in Aquatic Sciences*, v. 4, p. 411–447.
- Balsam, W., Damuth, J.E., and Deaton, B., 2007, Marine sediment components: identification and dispersal assessed by diffuse reflectance spectrophotometry: *International Journal of Environment and Health*, v. 1, p. 403–426, doi:10.1504/IJENVH.2007.017869.
- Barber, D.C. et al., 1999, Forcing of the cold event of 8,200 years ago by catastrophic drainage of Laurentide lakes: *Nature*, v. 400, p. 344–348, doi:10.1038/22504.
- Barranco, F.T., Balsam, W.L., and Deaton, B.C., 1989, Quantitative reassessment of brick red lutites: Evidence from reflectance spectrophotometry: *Marine Geology*, v. 89, p. 299–314, doi:10.1016/0025-3227(89)90082-0.
- Blum, P., 1997, *Physical Properties Handbook: A Guide to the Shipboard Measurement of Physical Properties of Deep-Sea Cores: Ocean Drilling Program, Ocean Drilling Program Technical Notes*, doi:10.2973/odp.tn.26.1997.
- Böhm, E. et al., 2015, Strong and deep Atlantic meridional overturning circulation during the last glacial cycle: *Nature*, v. 517, p. 73–76, doi:10.1038/nature14059.

- Bond, G., Broecker, W., Lotti, R., and McManus, J., 1992, Abrupt color changes in isotope stage 5 in north Atlantic deep sea cores: implications for rapid change of climate-drive events, *in* Kukla, G.J. ed., *Start of a Glacial*, p. 185, doi:10.15713/ins.mmj.3.
- Bourne, M.D., Thomas, A.L., Niocail, C.M., and Henderson, G.M., 2012, Improved determination of marine sedimentation rates using ^{230}Th : *Geochemistry, Geophysics, Geosystems*, v. 13, p. 1–9, doi:10.1029/2012GC004295.
- Boyle, E.A., 2000, Is ocean thermohaline circulation linked to abrupt stadial/interstadial transitions? *Quaternary Science Reviews*, v. 19, p. 255–272, doi:10.1016/S0277-3791(99)00065-7.
- Channell, J.E.T., Hodell, D.A., Romero, O., Hillaire-Marcel, C., de Vernal, A., Stoner, J.S., Mazaud, A., and Röhl, U., 2012, A 750-kyr detrital-layer stratigraphy for the North Atlantic (IODP Sites U1302-U1303, Orphan Knoll, Labrador Sea): *Earth and Planetary Science Letters*, v. 317–318, p. 218–230, doi:10.1016/j.epsl.2011.11.029.
- Chough, S., and Hesse, R., 1976, Submarine meandering thalweg and turbidity currents flowing for 4,000 km in the Northwest Atlantic Mid-Ocean Channel, Labrador Sea: *Geology*, v. 4, p. 529–533.
- Dalton, A.S. et al., 2020, An updated radiocarbon-based ice margin chronology for the last deglaciation of the North American Ice Sheet Complex: *Quaternary Science Reviews*, v. 234, p. 106223, doi:10.1016/j.quascirev.2020.106223.
- Dyer, B., Austermann, J., D'Andrea, W.J., Creel, R.C., Sandstrom, M.R., Cashman, M., Rovere, A., and Raymo, M.E., 2021, Sea-level trends across The Bahamas constrain peak last interglacial ice melt: *Proceedings of the National Academy of Sciences*, v. 118, doi:10.1073/pnas.2026839118.
- Ewing, M., Heezen, B.C., Ericson, D., Northrop, J., and Dorman, J., 1953, Exploration of the northwest Atlantic mid-ocean canyon: *Geological Society of America Bulletin*, v. 64, p. 865–868.
- Flower, B., 1998, Mid-to late Quaternary stable isotopic stratigraphy and paleoceanography at Site 919 in the Irminger Basin: *Proceedings of the Ocean Drilling Program. Scientific Results*, v. 152, p. 243–248.
- Francois, R., and Bacon, M.P., 1994, Heinrich events in the North Atlantic: radiochemical evidence: *Deep-Sea Research Part I*, v. 41, p. 315–334, doi:10.1016/0967-0637(94)90006-X.
- Galaasen, E.V., Ninnemann, U.S., Irvall, N., Kleiven, H.F., Rosenthal, Y., Kissel, C., and Hodell, D.A., 2014, Rapid Reductions in North Atlantic Deep Water During the Peak of the Last Interglacial Period: *Science*, v. 343, p. 1129–1132, doi:10.1126/science.1248667.

- GEBCO Bathymetric Compilation Group, 2019, The GEBCO_2019 Grid - a continuous terrain model of the global oceans and land.; doi:10.5285/836F016A-33BE-6DDC-E053-6C86ABC0788E.
- GEBCO Sub-Committee on Undersea Feature Names, 2015, IHO-IOC GEBCO Gazetteer of Undersea Feature Names.; www.gebco.net (accessed February 2021).
- Giosan, L., Flood, R.D., and Aller, R.C., 2002a, Paleooceanographic significance of sediment color on western North Atlantic drifts: I. Origin of color: *Marine Geology*, p. 17.
- Giosan, L., Flood, R.D., and Gru, J., 2002b, Paleooceanographic significance of sediment color on western North Atlantic Drifts: II. Late Pliocene-Pleistocene sedimentation: *Marine Geology*, p. 19.
- Giosan, L., Flood, R.D., Grützner, J., Franz, S.O., Poli, M.-S., and Hagen, S., 2001, 6. HIGH-RESOLUTION CARBONATE CONTENT ESTIMATED FROM DIFFUSE SPECTRAL REFLECTANCE FOR LEG 172 SITE: Ocean Drilling Program, Proceedings of the Ocean Drilling Program, v. 172, doi:10.2973/odp.proc.sr.172.2001.
- Grützner, J. et al., 2002, Astronomical age models for Pleistocene drift sediments from the western North Atlantic (ODP Sites 1055–1063): *Marine Geology*, v. 189, p. 5–23, doi:10.1016/S0025-3227(02)00320-1.
- Hesse, R., Klauke, I., Khodabakhsh, S., and Ryan, W.B.F., 1997, Glacimarine Drainage Systems in Deep-sea: The NAMOC System of the Labrador Sea and its Sibling., *in* Davies, T.A., Bell, T., Cooper, A.K., Josenhans, H., Polyak, L., Solheim, A., Stoker, M.S., and Stravers, J.A. eds., *Glaciated Continental Margins: An Atlas of Acoustic Images*, Dordrecht, Springer Netherlands, p. 286–289, doi:10.1007/978-94-011-5820-6_95.
- Hesse, R., and Rakofsky, A., 1992, Deep-sea channel/submarine-Yazoo System of the Labrador Sea: a new deep-water facies model: *AAPG Bulletin*, v. 76, p. 680–707.
- Hillaire-Marcel, C., Aksu, A., Causse, C., de Vernal, A., and Ghaleb, B., 1990, Response of Th/U in deep Labrador Sea sediments (ODP Site 646 to changes in sedimentation rates and paleoproductivities: *Geology*, v. 18, p. 162–165, doi:10.1130/0091-7613(1990)018<0162:ROTUID>2.3.CO;2.
- Hodell, D.A., Minth, E.K., Curtis, J.H., McCave, I.N., Hall, I.R., Channell, J.E.T., and Xuan, C., 2009, Surface and deep-water hydrography on Gardar Drift (Iceland Basin) during the last interglacial period: *Earth and Planetary Science Letters*, v. 288, p. 10–19, doi:10.1016/j.epsl.2009.08.040.
- Hume, L.D., 2018, *The Last Interglacial in the Labrador Sea*: University of East Anglia.
- Irvali, N., Ninnemann, U.S., Galaasen, E.V., Rosenthal, Y., Kroon, D., Oppo, D.W., Kleiven, H.F., Darling, K.F., and Kissel, C., 2012, Rapid switches in subpolar North Atlantic hydrography

- and climate during the Last Interglacial (MIS 5e): *Paleoceanography*, v. 27, p. n/a-n/a, doi:10.1029/2011PA002244.
- Jennings, A., Andrews, J., Pearce, C., Wilson, L., and Ólfasdóttir, S., 2015, Detrital carbonate peaks on the Labrador shelf, a 13-7ka template for freshwater forcing from the Hudson Strait outlet of the Laurentide Ice Sheet into the subpolar gyre: *Quaternary Science Reviews*, v. 107, p. 62–80, doi:10.1016/j.quascirev.2014.10.022.
- Jennings, A.E., Manley, W.F., MacLean, B., and Andrews, J.T., 1998, Marine evidence for the last glacial advance across eastern Hudson Strait, eastern Canadian arctic: *Journal of Quaternary Science*, v. 13, p. 501–514, doi:10.1002/(SICI)1099-1417(1998110)13:6<501::AID-JQS391>3.0.CO;2-A.
- Keigwin, L.D., 2001, 9. DATA REPORT: LATE PLEISTOCENE STABLE ISOTOPE STUDIES OF ODP SITES 1054, 1055, AND 1063: Ocean Drilling Program, *Proceedings of the Ocean Drilling Program*, v. 172, doi:10.2973/odp.proc.sr.172.2001.
- Kerwin, M.W., 1996, A Regional Stratigraphic Isochron (ca. 8000 ¹⁴C yr B.P.) from Final Deglaciation of Hudson Strait: *Quaternary Research*, v. 46, p. 89–98, doi:10.1006/qres.1996.0049.
- Klaucke, I., Hesse, R., and Ryan, W.B.F., 1998, Seismic stratigraphy of the Northwest Atlantic Mid-Ocean Channel: growth pattern of a mid-ocean channel-levee complex: *Marine and Petroleum Geology*, v. 15, p. 575–585, doi:10.1016/S0264-8172(98)00044-0.
- Kopp, R.E., Simons, F.J., Mitrovica, J.X., Maloof, A.C., and Oppenheimer, M., 2009, Probabilistic assessment of sea level during the last interglacial stage: *Nature*, v. 462, p. 863–867, doi:10.1038/nature08686.
- Krastel, S., and Mosher, D., 2022, Mapping a River Beneath the Sea: *Eos*, v. 103, doi:10.1029/2022EO220052.
- Lambeck, K., Rouby, H., Purcell, A., Sun, Y., and Sambridge, M., 2014, Sea level and global ice volumes from the Last Glacial Maximum to the Holocene: *Proceedings of the National Academy of Sciences*, v. 111, p. 15296–15303, doi:10.1073/pnas.1411762111.
- Leng, W., von Dobeneck, T., Bergmann, F., Just, J., Mulitza, S., Chiessi, C.M., St-Onge, G., and Piper, D.J.W., 2018, Sedimentary and rock magnetic signatures and event scenarios of deglacial outburst floods from the Laurentian Channel Ice Stream: *Quaternary Science Reviews*, v. 186, p. 27–46, doi:10.1016/j.quascirev.2018.01.016.
- Lisiecki, L.E., and Raymo, M.E., 2005, A Pliocene-Pleistocene stack of 57 globally distributed benthic $\delta^{18}\text{O}$ records: *Paleoceanography*, v. 20, p. 1–17, doi:10.1029/2004PA001071.
- Lochte, A.A., Repschläger, J., Kienast, M., Garbe-Schönberg, D., Andersen, N., Hamann, C., and Schneider, R., 2019, Labrador Sea freshening at 8.5 ka BP caused by Hudson Bay Ice

- Saddle collapse: *Nature Communications*, v. 10, p. 586, doi:10.1038/s41467-019-08408-6.
- McManus, J.F., Anderson, R.F., Broecker, W.S., Fleisher, M.Q., and Higgins, S.M., 1998, Radiometrically determined sedimentary fluxes in the sub-polar North Atlantic during the last 140,000 years: *Earth and Planetary Science Letters*, v. 155, p. 29–43, doi:10.1016/S0012-821X(97)00201-X.
- Nicholl, J.A.L., Hodell, D.A., Naafs, B.D.A., Hillaire-Marcel, C., Channell, J.E.T., and Romero, O.E., 2012, A Laurentide outburst flooding event during the last interglacial period: *Nature Geoscience*, v. 5, p. 901–904, doi:10.1038/ngeo1622.
- Oppo, D.W., Keigwin, L.D., McManus, J.F., and Cullen, J.L., 2001, Persistent suborbital climate variability in marine isotope stage 5 and termination II: *Paleoceanography*, v. 16, p. 280–292, doi:10.1029/2000PA000527.
- Oppo, D.W., McManus, J.F., and Cullen, J.L., 2006, Evolution and demise of the Last Interglacial warmth in the subpolar North Atlantic: *Quaternary Science Reviews*, v. 25, p. 3268–3277, doi:10.1016/j.quascirev.2006.07.006.
- Paillard, D., Labeyrie, L., and Yiou, P., 1996, Macintosh Program performs time-series analysis: *Eos, Transactions American Geophysical Union*, v. 77, p. 379–379, doi:10.1029/96EO00259.
- Rashid, H., Hesse, R., and Piper, D.J.W., 2003a, Distribution, thickness and origin of Heinrich layer 3 in the Labrador Sea: *Earth and Planetary Science Letters*, v. 205, p. 281–293, doi:10.1016/S0012-821X(02)01047-6.
- Rashid, H., Hesse, R., and Piper, D.J.W., 2003b, Evidence for an additional Heinrich event between H5 and H6 in the Labrador Sea: *Paleoceanography*, v. 18, p. 1–15, doi:10.1029/2003PA000913.
- Skene, K.I., Piper, D.J.W., and Hill, P.S., 2002, Quantitative analysis of variations in depositional sequence thickness from submarine channel levees: *Sedimentology*, v. 49, p. 1411–1430, doi:10.1046/j.1365-3091.2002.00506.x.
- Smith, M., Glick, E., Lodestro, S., and Rashid, H., 2013, Data report: oxygen isotopes and foraminifer abundance record for the last glacial–interglacial cycle and marine isotope Stage 6 at IODP Site U1313: *Proceedings of Integrated Ocean Drilling Program*, v. 303, p. 306.
- Stoner, J.S., Channell, J.E.T., and Hillaire-Marcel, C., 1996, The magnetic signature of rapidly deposited detrital layers from the deep Labrador Sea: Relationship to North Atlantic Heinrich layers: *Paleoceanography*, v. 11, p. 309–325, doi:10.1029/96PA00583.

- St-Onge, G., and Lajeunesse, P., 2007, Flood-Induced Turbidites From Northern Hudson Bay And Western Hudson Strait: A Two-Pulse Record Of Lake Agassiz Final Outburst Flood?, *in* Lykousis, V., Sakellariou, D., and Locat, J. eds., *Submarine Mass Movements and Their Consequences*, Dordrecht, Springer Netherlands, p. 129–137, doi:10.1007/978-1-4020-6512-5_14.
- Tarasov, L., Dyke, A.S., Neal, R.M., and Peltier, W.R., 2012, A data-calibrated distribution of deglacial chronologies for the North American ice complex from glaciological modeling: *Earth and Planetary Science Letters*, v. 315–316, p. 30–40, doi:10.1016/j.epsl.2011.09.010.
- Thomas, E.R., Wolff, E.W., Mulvaney, R., Steffensen, J.P., Johnsen, S.J., Arrowsmith, C., White, J.W.C., Vaughn, B., and Popp, T., 2007, The 8.2ka event from Greenland ice cores: *Quaternary Science Reviews*, v. 26, p. 70–81, doi:10.1016/j.quascirev.2006.07.017.
- Tzedakis, P.C. et al., 2018, Enhanced climate instability in the North Atlantic and southern Europe during the Last Interglacial: *Nature Communications*, v. 9, p. 4235, doi:10.1038/s41467-018-06683-3.